Phytochemistry 69 (2008) 1962–1972

Contents lists available at ScienceDirect

Phytochemistry

journal homepage: www.elsevier.com/locate/phytochem

Hydroponic isotope labelling of entire plants (HILEP) for quantitative plant proteomics; an oxidative stress case study

Laurence V. Bindschedler [a,b,*], Magnus Palmblad [a,c], Rainer Cramer [a,d,*]

[a] The BioCentre, The University of Reading, P.O. Box 221, Reading RG6 6AS, United Kingdom
[b] The BioCentre, The University of Reading, Whiteknights, P.O. Box 221, Reading RG6 6AS, United Kingdom
[c] Department of Parasitology, Leiden University Medical Center, P.O. Box 9600, 2300 RC Leiden, The Netherlands
[d] Department of Chemistry, The University of Reading, P.O. Box 224, Reading RG6 6AD, United Kingdom

ARTICLE INFO

Article history:
Received 4 February 2008
Received in revised form 1 April 2008
Available online 5 June 2008

Keywords:
Quantitative proteomics
Metabolic labelling
Mass spectrometry
Protein expression
Oxidative stress
Hydroponics

ABSTRACT

Hydroponic isotope labelling of entire plants (HILEP) is a cost-effective method enabling metabolic labelling of whole and mature plants with a stable isotope such as ^{15}N. By utilising hydroponic media that contain ^{15}N inorganic salts as the sole nitrogen source, near to 100% ^{15}N-labelling of proteins can be achieved. In this study, it is shown that HILEP, in combination with mass spectrometry, is suitable for relative protein quantitation of seven week-old *Arabidopsis* plants submitted to oxidative stress. Protein extracts from pooled ^{14}N- and ^{15}N-hydroponically grown plants were fractionated by SDS–PAGE, digested and analysed by liquid chromatography electrospray ionisation tandem mass spectrometry (LC–ESI–MS/MS). Proteins were identified and the spectra of $^{14}N/^{15}N$ peptide pairs were extracted using their m/z chromatographic retention time, isotopic distributions, and the m/z difference between the ^{14}N and ^{15}N peptides. Relative amounts were calculated as the ratio of the sum of the peak areas of the two distinct ^{14}N and ^{15}N peptide isotope envelopes. Using Mascot and the open source trans-proteomic pipeline (TPP), the data processing was automated for global proteome quantitation down to the isoform level by extracting isoform specific peptides. With this combination of metabolic labelling and mass spectrometry it was possible to show differential protein expression in the apoplast of plants submitted to oxidative stress. Moreover, it was possible to discriminate between differentially expressed isoforms belonging to the same protein family, such as isoforms of xylanases and pathogen-related glucanases (PR 2).

1. Introduction

Quantitative analysis by mass spectrometry (MS) is a major challenge in proteomics as the correlation between analyte concentration and signal intensity is often poor due to varying ionisation efficiencies in the presence of molecular competitors. The two widely used ionisation techniques in biological MS, electrospray ionisation (ESI) and matrix-assisted laser desorption/ionisation (MALDI), suffer from this limitation, although various sample preparations, ion formation and data acquisition strategies have been devised for reducing these variations (Fang et al., 2006; Palmblad and Cramer, 2007; Tang et al., 2004).

Other strategies employed to circumvent this limitation include differential sample labelling and the introduction of well-defined references. For instance, sample spiking with a defined amount of an internal standard that is chemically identical but labelled with different isotopes allows the Absolute QUAntitation (AQUA) of a specific peptide (Gerber et al., 2003). In general, this method relies on the assumption that isotopically different internal standards have ionisation behaviours/efficiencies identical to the analyte. The obvious drawback of this approach, however, is the requirement of knowing the analyte to quantify in order to synthesise the isotopic standard. It is therefore not optimal for early discovery proteomics and relatively costly for large-scale analyses (Wienkoop and Weckwerth, 2006).

Nevertheless, numerous methods for relative quantitation by comparing two or more samples are available, for instance by comparing spot intensities of proteins separated electrophoretically on silver- or Coomassie-stained gels. This technique has several disadvantages, including the individual treatment of samples, and thus introducing sample-to-sample variability. In addition, silver or Coomassie staining has a limited dynamic range for quantitative analysis, and staining intensities are dependent on the nature of the proteins. To overcome these problems, the derivatisation of proteins with fluorescent dyes such as CyDyes™ has been

* Corresponding authors. Address: The BioCentre, The University of Reading, Whiteknights, P.O. Box 221, Reading RG6 6AS, United Kingdom. Tel.: +44 1183784564; fax: +44 1183784551 (L.V. Bindschedler); Tel.: +44 1183784550; fax: +44 1183784551 (R. Cramer).
E-mail addresses: l.v.bindschedler@reading.ac.uk (L.V. Bindschedler), r.k.cramer@reading.ac.uk (R. Cramer).

0031-9422/$ - see front matter © 2008 Elsevier Ltd. All rights reserved.
doi:10.1016/j.phytochem.2008.04.007

introduced to improve the relative quantitation of proteins by pooling the individually labelled samples prior to protein separation (Marouga et al., 2005; Unlu et al., 1997).

Relative quantitation methods that utilise differential stable isotope labelling coupled to mass spectrometric detection are alternatives to chromophore labelling. Isotope Coded Affinity Tag (ICAT) uses two differential mass tags ($^{12}C_9$ and $^{13}C_9$ isotope labels), which specifically bind to cysteine-containing peptides that can then be purified through the incorporated biotin moiety (Yi et al., 2005). The difference of 9 Da per cysteine is detectable by MS and the differential ion intensities are used for relative quantitation. Similarly, the recently introduced isotope coded protein labelling (ICPL) method (Schmidt et al., 2005) allows the differential isotope labelling of free amino groups, e.g. on lysines.

While ICAT and ICPL use the ion intensity of precursor ions, i.e. of the first-stage mass spectrometric read-out, for quantitation, isobaric tags for relative and absolute quantitation (iTRAQ) exploits the specific design of different tags of identical mass, each of which yields a unique low-mass reporter ion in MS/MS, enabling relative quantitation between up to 8 of such labelled samples (Ross et al., 2006, 2004b). As well as allowing high multiplexing capability, iTRAQ and ICPL label the more abundant lysine residues, thus avoiding the lower proteome coverage resulting from cysteine labelling techniques. Although either of the above techniques are suitable for labelling at the protein level before proteolysis, the initial preparative steps prior to these (e.g. protein extraction and pre-fractionation) may lead to systematic errors.

The drawbacks inherent to chemical labelling methods can be overcome by metabolic labelling with amino acids containing stable isotopes (e.g. ^{13}C and/or ^{15}N). In stable isotope labelling with amino acids in cell culture (SILAC) (Mann, 2006), cells are typically grown in the presence of $^{12}C/^{14}N$, $^{13}C/^{14}N$, $^{12}C/^{15}N$ or $^{13}C/^{15}N$ arginine. SILAC has also been used to label proteins in *Arabidopsis* cell cultures, but because plants can fix carbon from atmospheric CO_2, complete labelling is prevented (Gruhler et al., 2005). In addition, although whole plants can be grown using amino acids as sole nitrogen source (Hirner et al., 2006), applying SILAC to whole *Arabidopsis* plants is expensive.

Alternative methods to SILAC for metabolic labelling with ^{15}N or ^{13}C have been developed (for review see (Heck and Krijgsveld, 2004)), for instance for cultures of *E. coli* (Ross et al., 2004a), mammalian cells (Conrads et al., 2001) and yeast (Kolkman et al., 2006). In these cases, the media contained mixed organic and inorganic nitrogen sources, but it was estimated to contain 98–99% ^{15}N supplied as ammonium and/or nitrate inorganic salt. However, these inexpensive ^{15}N-labelling studies were subject to differential protein expression due to nitrogen limitation (Kolkman et al., 2006) or utilised additional nitrogen sources (Conrads et al., 2001). Whole organisms such as *C. elegans* and *Drosophila melanogaster* were fed on ^{15}N *E. coli* and yeast for metabolic labelling (Krijgsveld et al., 2003), and rats were ^{15}N-labelled through a protein-free diet supplemented with ^{15}N algal cells (Wu et al., 2004). More recently, *Arabidopsis* cell cultures were labelled with ^{15}N in a medium containing inorganic nitrate as the sole nitrogen source to quantitate proteins and nitrogen-containing metabolites (Benschop et al., 2007; Engelsberger et al., 2006) and young seedlings grown in shaking liquid cultures (Huttlin et al., 2007; Nelson et al., 2007).

Hydroponic metabolic ^{15}N-labelling has been used to label whole potato plants for structural analysis of abundant tuber proteins by NMR (Ippel et al., 2004). Hydroponic labelling with inexpensive media enables the quantitative analysis at the molecular level of whole plants responding to environmental stimuli or diseases, since hydroponic culturing is ideal to undertake metabolic labelling under well-controlled plant growth conditions.

In this paper, we demonstrate the suitability of metabolic ^{15}N hydroponic isotope labelling of entire plants (HILEP) for relative quantitative proteomic analysis by mass spectrometry as illustrated with *Arabidopsis* plants subjected to oxidative stress. It has been previously shown that reactive oxygen species (ROS) are produced following various biotic and abiotic stresses (for review see (Apel and Hirt, 2004; Neill et al., 2002)) which induce the expression of many transcripts (Baxter et al., 2007) and proteins, including the extracellular pathogenesis-related (PR) proteins (van Loon et al., 2006). Moreover, extracellular hydrogen peroxide production by apoplastic peroxidase(s) is involved in the induction of plant defence to various pathogens (Bindschedler et al., 2006).

For the routine application of HILEP in an integrated, easy-to-apply and robust analytical workflow, we have developed and adapted an automated data analysis pipeline using mzXML (http://tools.proteomecenter.org/mzXMLshema.php), Mascot (http://www.matrixscience.com) and the trans-proteomic pipeline (TPP) (http://tools.proteomecenter.org/software.php) based on the data processing workflow recently described in detail (Palmblad et al., 2007).

2. Results

2.1. Labelling and treatment of whole arabidopsis plants grown in hydroponic culture

Metabolic ^{15}N-HILEP of *Arabidopsis thaliana* was achieved by growing plants in a hydroponic medium where the ammonium and nitrate were replaced by the equivalent ^{15}N-labelled nitrogen sources. Ammonium was maintained in the medium as it has been reported to produce healthy looking plants with bigger leaves (Tocquin et al., 2003). No phenotypic differences were observed between hydroponically grown ^{15}N and ^{14}N plants (Fig. 1). Thus, this culture system is convenient for the study and the relative quantitation of proteins from the proteome of whole mature plants under well-defined physiological growth conditions minimising experimental variations, for instance, due to soil composition and watering frequency.

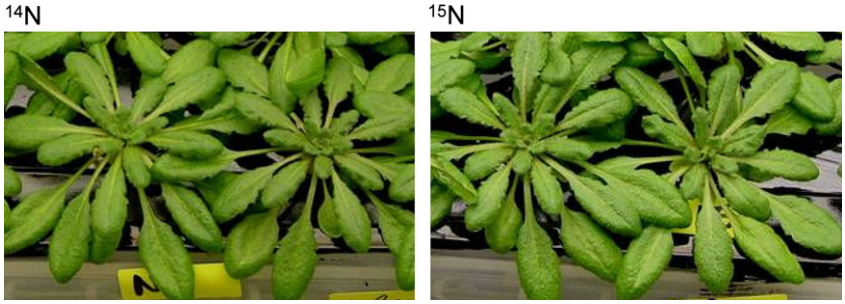

Fig. 1. Seven week-old plants grown hydroponically. No phenotypic differences could be detected between plants grown in ^{14}N or ^{15}N inorganic salts.

The percentage of incorporated ^{15}N was estimated in the isotopic envelope of ^{15}N-labelled proteolytic peptides by adopting the method for calculating deuterium incorporation in hydrogen/deuterium exchange mass spectrometry (Palmblad et al., 2001). Five randomly chosen peptide ion signals from the large subunit of Rubisco (AtCg00490) quantified by FTICR–MS gave a level of ^{15}N incorporation of 98.1 ± 0.1% (Fig. 2), which is consistent with the manufacturers' specifications of the ^{15}N content of the potassium nitrate (99% ^{15}N) and ammonium nitrate (98% ^{15}N) provided by the labelled hydroponic medium. The ^{14}N isotopic distribution pattern of a given peptide from a 1:1 (w:w) $^{14}N/^{15}N$ pooled sample was identical to that same peptide from a non-mixed ^{14}N (unlabelled) sample, and the ^{14}N and ^{15}N isotopic envelopes of the corresponding ^{14}N and ^{15}N peptides did not overlap (Fig. 3a). For most peptides the mass difference between the ^{14}N monoisotopic peak and the most abundant ^{15}N isotopic peak was in good agreement with the calculated theoretical number of nitrogen atoms (see, for instance, Fig. 3a). The MS/MS spectra of the corresponding ^{14}N and ^{15}N peptides were similar (see, for instance, Fig. 3b). In addition, these peptides co-eluted from the LC system. Thus retention time, m/z difference between ^{14}N and ^{15}N isotope pairs and the similarity of ^{14}N and ^{15}N MS/MS spectra can be used for protein identification and $^{14}N/^{15}N$ peptide pairing. The relative peptide amounts were calculated as the ratio of the sums of the heavy and light isotope peak areas.

2.2. Protein fractionation, LC separation, protein identification and manual quantitation

To establish and evaluate HILEP for quantitative proteomics, *Arabidopsis* leaves from plants grown in ^{14}N and ^{15}N hydroponic media were pooled in a 1:3.5 (w:w) $^{14}N:^{15}N$ ratio. Total protein extracts were digested with trypsin and analysed by LC–ESI–MS/MS for manual quantitation. The average (3.58 ± 0.45) of manually measured $^{14}N/^{15}N$ peptide ratios for the large subunit of Rubisco (AtCg00490) reflected the expected 1:3.5 (w:w) ratio (Table 1).

Then *Arabidopsis* plants were submitted to oxidative stress by treatment with H_2O_2 for comparison with non-treated plants. Leaves from treated and control plants were pooled in 1:1 ratio (w:w) prior to protein extraction and fractionation by 1D SDS–PAGE. Proteins were quantified manually from a total protein extract (30 h after treatment) and from intercellular washing fluids (IWFs, 40 h after treatment) enriched in extracellular apoplastic proteins prior to the analysis of independent samples for setting up the automated workflow for global proteome analysis (see next section). Total extracts were chosen as they are complex samples, enabling the testing of the robustness of the quantitation method. IWFs were chosen as many stress-induced proteins are known to be secreted in the intercellular apoplastic space 1–3 days after various abiotic stresses generating reactive oxygen species (ROS). Treated plants were ^{14}N-grown whereas control samples were ^{15}N-grown. The abundant Rubisco large subunit (labelled "R" in Fig. 4a) was used as a marker protein during method development and as a quantitation reference as it was present as a contaminant in the IWFs and its level was not influenced by the H_2O_2 treatment.

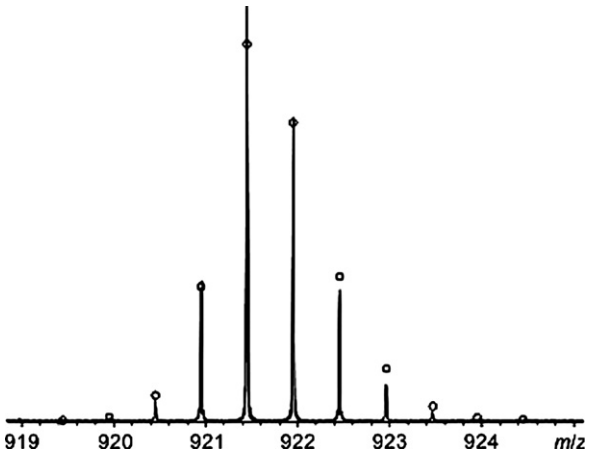

Fig. 2. Comparison of the experimental FTICR mass spectral data with the theoretical isotope pattern for the peptide LEGDRESTLGFVDLLR (AtCg00490, Rubisco fragment 335–350) to estimate the % of ^{15}N incorporation. Least-squares fit (circles) for the theoretical data was obtained according to the method described by Palmblad et al. (2001), substituting ^{2}H incorporation for ^{15}N as the independent variable (98.1 ± 0.1% ^{15}N).

To avoid quantitation errors due to overlapping isotopes of different ion species with a similar m/z and because Rubisco accounts for more than 40% of the total leaf protein amount (McCabe et al., 2001), protein pre-fractionation of leaf extracts proved to be beneficial. Without pre-fractionation, as in the analysis of total extracts, virtually only Rubisco (AtCg00490) and a few other abundant proteins were identified (data not shown). Thus proteins were separated on 1D SDS–PAGE (Fig. 4).

Due to the complexity of the samples, a high-capacity ion trap mass spectrometer with fast scan times in MS/MS mode was chosen. The resulting high number of MS/MS spectra per protein enabled the identification and matching of ^{15}N-labelled peptides to the corresponding ^{14}N peptides solely by comparison of their MS/MS spectra (Fig. 3b).

To evaluate the suitability of HILEP technology for protein quantitation, IWF protein extracts collected 40 h post treatment were separated on SDS–PAGE (Fig. 4a, Tables 2 and S1). Image analysis revealed differential staining of several bands between control and treated samples (Fig. 4a, white dots). Of these, five corresponding bands from the pooled sample, including a band containing Rubisco (1–4, R, Fig. 4a) were excised for analysis. From the five bands, 82 unique proteins were identified with 95% probability and at least 3 unique peptides in Mascot (Table S1). Most of these proteins are known to be extracellular proteins such as various glycosyl hydrolases, including PR2 glucanases, PR3 chitinases and xylosidases, a serine protease, lectin-like proteins, lipases or lipid transfer proteins, a catalase (CAT2), two secretory peroxidases (P52 and P71) and two putative disease resistance proteins (At4g33300; At1g33590), (Table S1). The ^{14}N (treated)/^{15}N (control) ratios of 124 peptides assigned to 20 of the identified proteins were calculated manually (see Tables 2 and S1). Within this small set of proteins quantified manually, it was possible to measure $^{14}N/^{15}N$ ratios between 0.45 and 5.4. As expected, many of these proteins (12 out of 24) were significantly differentially expressed (Table 2). For instance two chitinases (PR3), a glucanase (PR2) and PR5 were up-regulated while a blue copper binding protein, a pectin esterase and a β-xylosidase were down-regulated following H_2O_2 treatment (Table 2).

The error on relative protein quantitation using data generated with the ion trap mass spectrometer was estimated with the peptide ratio SD of each manually quantified protein. The peptide ratio SD was consistently lower when more peptides were used for protein quantitation. It was typically below 20% when proteins were quantified with 5 or more peptides. A similar correlation was observed when plotting the SD against the Mascot score (data not shown).

MS and MS/MS spectra were manually examined to investigate ion signal interference from overlapping ion species. In some cases, the ^{14}N and the ^{15}N isotope envelopes did not follow the expected isotope distributions due to overlapping ion signals from different peptide species with very close m/z values (Δ m/z of 0.1 or less) that can not be discriminated with an ion trap mass spectrometer (e.g. Fig. 5a). However the high resolving power of FTICR–MS

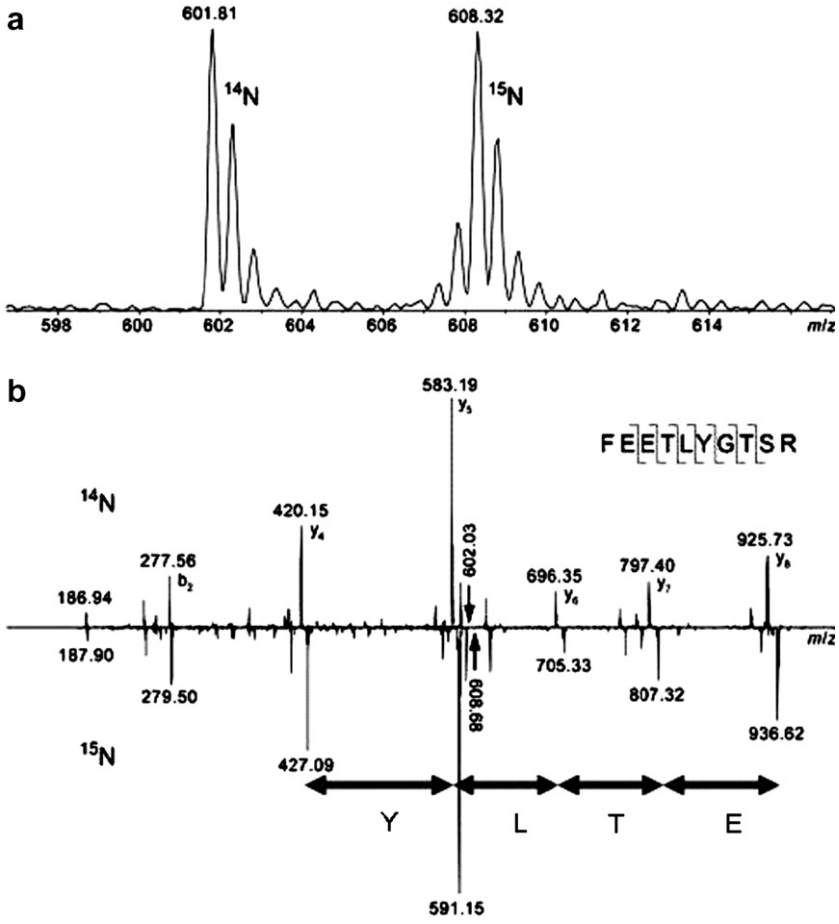

Fig. 3. Ion trap MS (a) and MS/MS (b) spectra of the sedoheptulose-bisphosphatase (Q940F8, At3g55800) peptide FEETLYGTSR containing 13 nitrogen atoms. Both the ^{14}N (m/z 602) and ^{15}N (m/z 608) peptide were selected for MS/MS. Their MS/MS spectra are shown in (b) above and below the m/z axis, respectively, with arrows indicating the precursor ions. Continuous b- and y-ion series can be observed for both peptides, showing the residue-dependent shift (equal to the number of nitrogen atoms in the fragment ion) between the ^{14}N and ^{15}N peptides.

Table 1
$^{15}N/^{14}N$ ratios measured manually for peptides of the large subunit of Rubisco (AtCg00490) from a 1:3.5 (w:w) ^{14}N:^{15}N protein extract pool

$^{15}N/^{14}N$ ratio	Peptide
4.15	R.AMHAVIDR.Q
4.15	K.DTDILAAFR.V
3.64	R.DLAVEGNEIIR.E
4.00	R.ESTLGFVDLLR.D
3.17	R.FLFCAEAIYK.S
3.51	K.EITFNFPTIDK.L
3.66	K.LTYYTPEYETK.D
3.95	R.LSGGDHIHAGTVVGK.L
4.10	K.TFQGPPHGIQVER.D
2.68	K.DDENVNSQPFMR.W
3.75	K.YGRPLLGCTIKPK.L
3.31	K.WSPELAAACEVWK.E
3.12	K.GHYLNATAGTCEEMIK.R
3.39	K.EITFNFPTIDKLDGQE.-
3.06	R.GGLDFTKDDENVNSQPFMR.W
3.58 ± 0.45	Measured average (±SD)
3.5	Expected average[a]

[a] The 1:3.5 ^{14}N:^{15}N pool was prepared by extracting proteins from 20 mg of ^{14}N-grown leaves pooled with 70 mg of ^{15}N-grown leaves.

enabled baseline resolution of different co-eluting peptide ion species with a $\Delta\ m/z < 0.03$. For instance, a peptide assigned to phosphoglycerate kinase with a monoisotopic ^{14}N m/z value of 553.29 had a mixed ^{15}N isotope envelope (Fig. 5b). Data from the ion trap mass spectrometer gave a $^{15}N/^{14}N$ ratio of 1.78 for this peptide whereas the average ratio for this particular protein was 1.13 ± 0.10 when the data for this peptide was excluded. In contrast to the ion trap data, the FTICR data revealed that different peptide species were present at the same nominal mass (Fig. 5c). $^{15}N/^{14}N$ ratios were thus more precise and SD values dropped below 10% when calculated from FTICR data (data not shown). However, because of the slower duty cycle of the FTICR in MS/MS mode, the ion trap was chosen for its speed to maximize amino acid sequence coverage and thus improving protein identification.

2.3. Automation of HILEP quantitation using the trans-proteomic pipeline (TPP)

To show the suitability of the HILEP technology for global quantitative analysis in a biological context, an experiment was designed to analyse the *Arabidopsis thaliana* proteome after oxidative stress. In this experiment, plants were treated as described for the experiment performed for the manual quantitation of proteins. Four different protein samples were extracted and separated by SDS–PAGE (total extracts and IWFs collected at two different time points: 20 h and 40 h post treatment, Fig. 4b and c). Treated plants were ^{14}N-grown whereas control samples were ^{15}N-grown. Whilst the aim of this paper is to demonstrate that the HILEP technology works in principle in a biological context, further replicates would be needed to determine the biological variation. However, comparable results were obtained when reciprocal

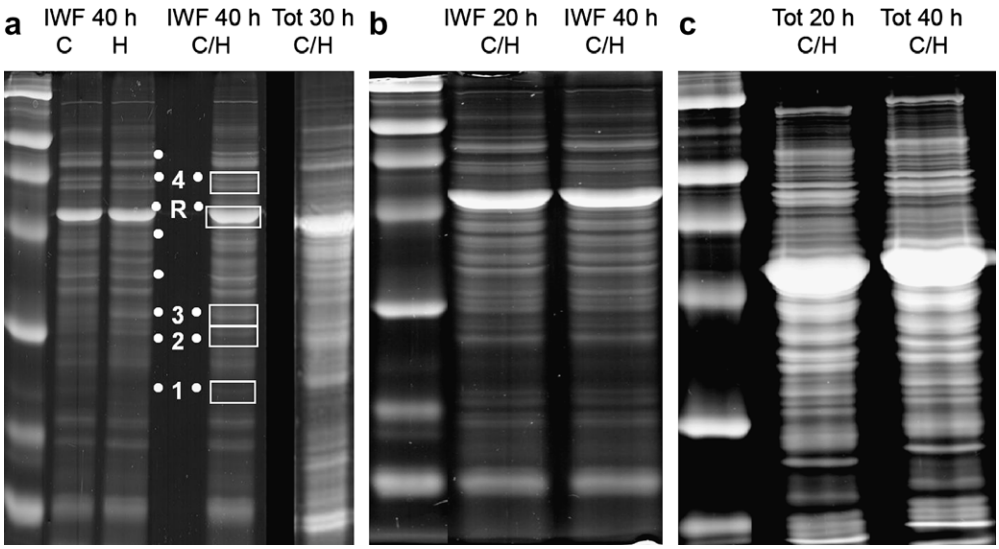

Fig. 4. Coomassie stained SDS–PAGE gels of apoplastic proteins from IWFs (5 μg, IWF) or total protein extracts (20 μg, Tot) from leaf material of control (C; ^{15}N) and 100 mM H_2O_2 (H; ^{14}N) treated plants or ^{14}N:^{15}N 1:1 pooled leaf material (C/H). (a) The gel image of IWFs from ^{15}N-labelled control plants (C) and unlabelled (^{14}N) 100 mM H_2O_2 treated plants (H) shows subtle expression differences as indicated by dots. The 5 gel bands 1–4 and R (containing Rubisco) of the (C/H) pool were excised for protein identification and quantitation; (b) Gel image of 20 h and 40 h C/H pooled IWF fractions; (c) Gel image of 20 h and 40 h C/H pooled total extracts. Twenty five gel bands from the 20 h and 40 h C/H pooled IWF and total protein extracts were excised for automated protein identification and quantitation.

Table 2
$^{15}N/^{14}N$ ratios calculated manually for proteins identified in the 1:1 control (^{15}N):H_2O_2 treated (^{14}N) 40 h IWF sample pool separated on SDS–PAGE (see Fig. 3A, gel bands 1–4 and R containing Rubisco)

		Ratio	SD	*t*-test	Nb Pep	Mascot score
At4g12880	Blue copper-binding protein, 15 K lamin	0.47	0.10	0.00	4	108
At5g64570	Beta-xylosidase	0.47	0.16	0.00	8	417
At1g76160	Pectinesterase putative Multicopper ox.	0.62	0.13	0.00	12	561
At1g29670	Lipase/hydrolase, putative	0.91	0.11	0.00	8	501
AtCg00490	Rubisco large SU	1.12	0.21	1.00	20	1354
At1g78060	Glycosyl hydrolase (3 and 3c)	1.36	0.64	0.46	5	191
AT5g25980	Thioglucosidase (EC 3.2.1.147)	1.49	0.35	0.08	5	356
At5g14740	Carbonic anhydrase 2	1.54	0.50	0.10	6	566
At1g75040	Pathogenesis-related protein 5 (PR-5)	1.57	0.25	0.00	10	608
At3g59970	Methylenetetrahydrofolate reductase	1.73	0.06	0.00	4	177
At1g33590	Putative disease resistance protein	1.77	0.32	0.04	4	314
At5g49360	Xylosidase	1.78	1.12	0.12	9	539
At4g09000	14-3-3 protein homolog GF14 chi chain	2.01	0.26	0.02	3	236
At1g06680	Oxygen-evolving complex protein 23 K	2.19	0.52	0.07	3	249
At5g09660	Malate dehydrogenase (EC 1.1.1.37)	2.28	1.25	0.07	6	319
At2g43620	Probable endochitinase [imported]	2.93	0.99	0.03	3	113
At3g57260	Glucan beta 1,3D glucosidase (PR2)	3.46	0.93	0.05	3	187
At5g66570	Oxygen evolving complex protein 33 K	3.73	1.58	0.10	3	288
At2g43570	Probable endochitinase	5.11	0.85	0.01	3	222
At3g14310	Pectinesterase	5.40	2.65	0.02	5	385

Significantly differentially regulated proteins (*t*-test; 95% probability) are highlighted in grey.

experiments were performed with ^{14}N-controls and ^{15}N-treated samples (data not shown). Also many of the differentially expressed proteins quantified manually where consistently differentially expressed in the replicated IWF 40 h sample of the automated analysis (Tables 2 and 3). Each gel lane was cut into 25 slices, followed by protein in-gel digestion and LC–MS/MS. From each gel slice 5–25 proteins were identified. Several hundred MS/MS spectra of unique peptides were acquired per gel band. IWF extracts typically lead to 100–150 protein identifications while 300 proteins were identified from the total extracts. For instance, from the 40 h total extract 312 protein identifications were retrieved with the TPP ProteinProphet tool while 112 were obtained for the 20 h IWF extract (Table S2).

TPP was adapted to allow the automated quantitation of $^{14}N/^{15}N$ peptide ratio calculation (see Materials and Methods and Fig. 6). This analytical workflow increased the speed and quality of analysis considerably, as peptide information from proteins that were present in adjacent gel slices analysed in repeated MS analyses or identified in the complimentary nitrogen pool could be merged. Moreover, quantitation data could be conveniently transferred to Excel for statistical analyses.

Although the TPP tool ProteinProphet is useful to fuse ^{14}N and ^{15}N data for protein identifications and peptide ratio averages, it was not possible to retrieve individual peptide ratios, thus preventing statistical analysis. Therefore, ProteinProphet was only used for a quick survey screen. Proteins were considered as putatively differentially expressed if the absolute difference between the expression ratio of the protein and the reference protein (Rubisco large subunit) was more than twice the SD. For example, in IWF extracts, lipases and lipid transfer proteins and several cell wall

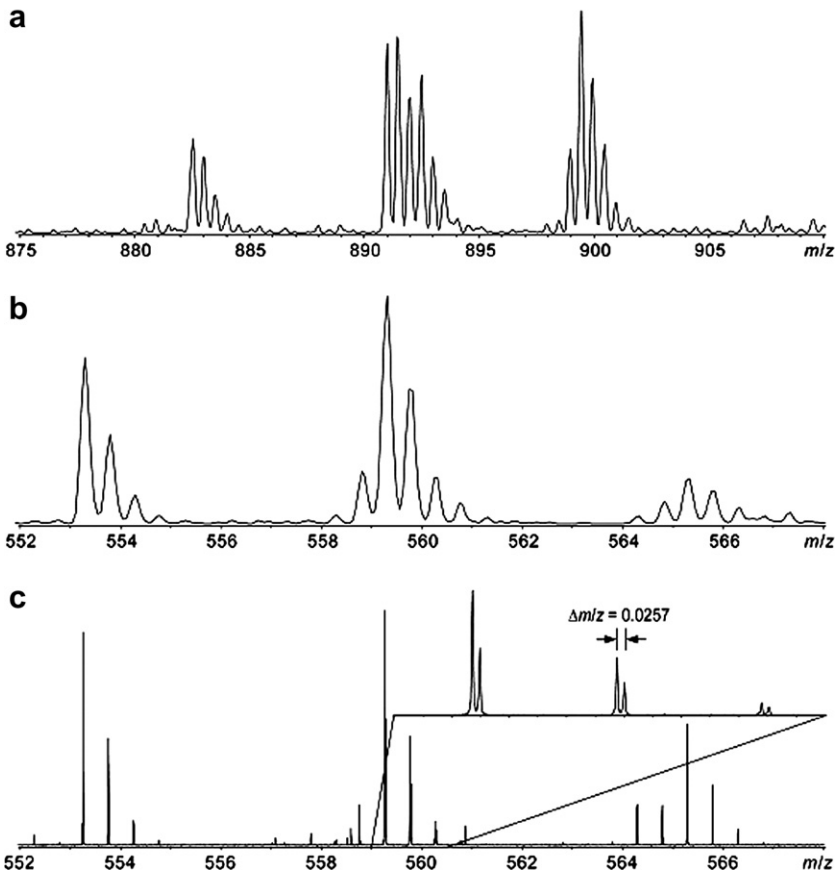

Fig. 5. Ion trap and FTICR mass spectra of overlapping ^{14}N and ^{15}N species as revealed by the isotope pattern. In (a), the ^{15}N envelope of the peptide EGPPVFEQPEMTYEK from Rubisco activase (At2g39730) is partially overlapping with the ^{14}N envelope of another peptide (unidentified). In other cases (e.g. SVGDLTSADLK from phosphoglycerate kinase; At3g12780), the mass difference is too small to be resolved or detected in an ion trap (b). Without correctly identifying the two flanking ^{14}N and ^{15}N (unidentified) peptides there would be no indication that two overlapping species are present in this spectrum. With a resolving power of 80,000, easily achieved in 7 tesla FTICR mass spectrometers, these two species, differing by 0.05 Da, are resolved to the baseline (c).

modifying enzymes seemed to be down-regulated, whereas several lectins, GSTs, endochitinases, pectinesterases and a peroxidase seemed to be induced in plants submitted to oxidative stress (Tables 3 and S2). However, PeptideProphet viewer was preferentially used to filter and export individual peptide data to Excel for subsequent statistical analysis.

Thus using the PeptideProphet tool, in the automated analytical workflow, solely isoform specific peptides were extracted to enable isoform specific quantitation of homologous proteins, using the same general requirement of a minimum of three peptides per protein. This is well illustrated by two β-1,3-glucanase isoforms detected in the IWF fraction, both belonging to the glycosyl-hydrolases family 17, one of which is significantly up-regulated (BG2, At3g57260) while the other is down-regulated (BG3, At3g57240), (Tables 3 and S3). The amino acid sequences of these two protein isoforms are 65% identical. The use of tryptic peptides common to both isoforms (e.g. (K)NGSPRR) would thus be a source of quantitation error. Despite the stringent criteria to selectively retrieve isoform specific data, 102 proteins with at least 3 isoform specific peptides could still be discriminately quantified at the isoform level for the 40 h total extract (Table S3). Similarly, in the 20 h IWF sample, out of the 112 proteins identified, 59 unique proteins were discriminatively quantified down to the isoform level (Table S3).

Thus, using the automated analytical workflow for discriminating protein isoforms, it was possible to observe significantly up- or down-regulated protein isoforms in the total extracts, including a heat shock protein (HSP 70), a NADP dependent malic enzyme-like protein and a putative isocitrate dehydrogenase (all up-regulated at 20 h). A calcium-dependent membrane binding annexin and a thylakoid luminal 19 kDa protein were significantly down-regulated at 20 h and 40 h, respectively (Table S3). Interestingly, annexin 1 protein isoform AnnAt1 (At1g35720) that was previously shown to have peroxidase activity and to be able to degrade hydrogen peroxide (Gorecka et al., 2005) was down-regulated. Significantly up- or down-regulated proteins from the IWF are presented in Table 3. For instance, it is noteworthy that two glyceraldehyde-3-P-dehydrogenase isoforms, a glucan-β-1,3-glucosidase (PR2), a secretory peroxidase (P71), two glutathione-S-transferases and a putative chitinase (PR3) were significantly up-regulated 20 h or 40 h after the H_2O_2 treatment, whereas for instance a subtilisin-like protease, an aspartyl-like protease, several lipases, a β-xylosidase, a β-1,3 glucanase, an α-galactosidase as well as β-like galactosidase and a pectinesterase were significantly down-regulated (Tables 3 and S3). Finally five of the differentially expressed protein isoforms described above were re-examined manually to validate the automation (underlined ratios shown in Table 3, 40 h time point). Manually calculated $^{14}N/^{15}N$ ratios for these proteins were consistent with automatically acquired data. In the case of the P71 secretory peroxidase isoform the $^{14}N/^{15}N$ ratio was 2.3 ± 0.25 for the automated quantitation but was 6.5 ± 4.17 for the manual quantitation. However, the ratios ± SD overlapped and the large SD for the manually quantified ratio is explained by the low ion signals of the identified ^{14}N peptides and the even lower or absent ion signals for the ^{15}N peptides of this protein (signal to noise ratio <5). Thus it is advisable to manually

Table 3
$^{15}N/^{14}N$ ratios calculated with the automation workflow (Fig. 6) for proteins from IWFs separated on SDS–PAGE (Fig. 3B)

TAIR	Name	20 h			20 h			40 h			40 h		
		^{14}N Id.		Nb	^{15}N Id.		Nb	^{14}N Id.		Nb	^{15}N Id.		Nb
		Ratio	SD	Pep	Ratio	SD	Pep	Ratio	SD	Pep	Ratio	SD	Pep
AtCg00490	RUBISCO large SU	1.00	0.34	18	1.00	0.27	15	1.02	0.17	28	0.93	0.18	25
At3g57240	Beta-1, 3-glucanase	0.42	0.05	6	0.47	0.23	10						
At5g64570	Beta-xylosidase	0.43	0.05	7	0.49	0.06	8	[a]0.69	0.10	6	0.69	0.11	5
At1g76160	Putative pectin esterase (copper oxidase)	0.45	0.03	4	0.45	0.03	5						
At3g16370	Proline-rich APG-like; GDSL-lipase[backslash]hydrolase-like protein				0.52	0.16	3						
At5g67360	Subtilisin-like (Cucumisin-like) serine protease	0.54	0.08	9	0.55	0.11	7	0.76	0.15	5	0.68	0.12	7
At1g35720	Annexin (Ca2+-dependent membrane-binding protein)				0.57	0.17	4						
At1g29660	Lipase[backslash]hydrolase, putative	0.58	0.04	3				0.73	0.07	4	0.73	0.07	4
At1g79720	Putative aspartyl protease				0.58	0.19	4						
At3g52840	Beta-galactosidase-like protein				0.58	0.18	4						
At1g21670	Putative TolB periplasmic component				0.58	0.04	7						
At3g18490	CND41, chloroplast nucleoid DNA binding protein-like				0.59	0.08	3	0.93	0.05	4			
At5g08380	Alpha-galactosidase-like protein				0.60	0.08	4						
At1g09750	Nucleoid DNA-binding-like protein							0.63	0.15	4	0.72	0.11	4
At2g28470	Putative beta-galactosidase				0.65	0.07	5						
At5g17920	Vitamin-B12-independent methionine synthase isozyme	0.73	0.06	6	0.74	0.27	9						
At1g29670	Lipase[backslash]hydrolase, putative	0.78	0.13	5				[a]0.75	0.17	7	0.79	0.07	7
At3g19170	Zinc metalloprotease 1, AtZnMP1 (AtPreP1)	0.76	0.10	3									
At4g33010	Putative glycine dehydrogenase-(P-protein 2)	0.78	0.01	3	0.79	0.10	4						
At3g57260	PR-2 Glucan endo-1,3-beta-glucosidase, acidic isoform							[a]1.27	0.09	6	1.24	0.08	6
At2g30860	Glutathione S-transferase							1.28	0.15	4			
At1g09340	Putative RNA-binding/Nucleoside diphosphate sugar epimerase	1.45	0.22	7				1.39	0.16	7			
At3g26650	Glyceraldehyde-3-phosphate dehydrogenase A, chloroplastic	1.48	0.28	4	1.85	0.29	3						
At1g42970	Glyceraldehyde-3-phosphate dehydrogenase B, chloroplastic	1.63	0.23	12	1.71	0.16	6	1.42	0.32	10	1.51	0.15	4
At4g02520	Glutathione S-transferase PM24 (GST class-phi)	1.67	0.28	3	1.37	0.17	3						
At3g12780	Phosphoglycerate kinase	1.91	0.36	4									
At2g43570	Endochitinase isolog (Putative endochitinase)							[a]2.08	0.22	3			
At4g05180	Oxygen-evolving enhancer protein 3–2, (OEE3, 16 K)	2.17	0.27	3									
At5g64120	Peroxidase 71 (Atperox P71, ATP15a, ATPO2)							[a]2.30	0.25	4			

Significantly differentially regulated proteins (Student *t*-test; 95% probability, ratios <0.8 and ratios >1.25) with at least 3 unique isoform specific peptides are shown.
[a]Underlined ratios were also calculated manually and consistent results were obtained, except for At5g64120 (see text). Manual ratios were 0.66 ± 0.07 (At5g64570), 0.79 ± 0.05 (At1g29670), 1.29 ± 0.12 (At3g57260), 2.17 ± 0.26 (At2g43570) and 6.5 ± 4.17(At5g64120).

check the quantitation of proteins with low ^{14}N or ^{15}N peptide signals. In conclusion, the automatic data analysis workflow proposed here is suitable for the quantitation of ^{15}N metabolically labelled proteins.

3. Discussion

Metabolic ^{15}N-labelling of proteins has been shown to be a powerful technique for quantitative proteomics of prokaryotes, yeast and multi-cellular organisms such as *C. elegans*, drosophila, mammals, plant cells (Benschop et al., 2007) and immersed plantlets in shaking cultures (Huttlin et al., 2007; Nelson et al., 2007). In this paper we have demonstrated that it is possible to label proteins of mature *Arabidopsis* plants to near completion using an inexpensive inorganic hydroponic solution containing $^{15}NO_3^-$ and $^{15}NH_4^+$ as the sole nitrogen sources. Moreover, the nitrogen concentration in the hydroponic solution is usually more than 10 times lower than in Murashige and Skoog derived cell culture media (Benschop et al., 2007; Huttlin et al., 2007; Nelson et al., 2007) which obviously reduces the cost per biomass produced considerably (circa £2.5 per g of leaf produced). Due to the low cost of the medium (£13/l), there is no need to label proteins with only a small fraction of ^{15}N. Consequently, isotopic envelopes of the natural and the cognate labelled peptide do not overlap, thus easing data processing (Huttlin et al., 2007). Furthermore, due to the absence of sucrose and a relatively low nitrogen concentration, the hydroponic medium is better suited to mimic natural plant growth in soil and HILEP allowed to grow and label healthy looking plants to full maturity (including seed production). In a biological context, we have shown that ^{15}N-HILEP coupled with mass spectrometry was suitable to detect and quantify protein expression variations due to oxidative stress in mature *Arabidopsis* plants. As this technology enables protein expression studies of whole organisms such as fully-grown plants, it is directly applicable to study more complex systems such as the protein expression during plant–pathogen interactions, including interactions with biotrophic pathogens. Therefore HILEP is far less limiting in its application than elicitors-cell culture systems (e.g. Chivasa et al., 2006).

As expected, in plants submitted to hydrogen peroxide, many more variations in protein expression were observed in the IWFs of leaf apoplasts in comparison with total leaf extracts. Several induced proteins have previously been shown to be induced in the IWFs following fungal or bacterial infection but also by various abiotic stresses leading to ROS production, e.g. the extracellular PR proteins such as chitinases from the PR-2 family, glucanases from the PR-3 family and a thaumatin-like protein from the PR-5 family (Dong et al., 1991; Ott et al., 2006; van Loon et al., 2006). The induction ratios of some proteins such as the beta-1,3-glucanase (PR-2) was higher in the initial pilot experimental set of manually quantified proteins (Table 1) compared to the second experiment where proteins were quantified automatically (Table 2). It is most likely that this is due to biological variations rather than analytical errors, since in the second experimental set, plants were treated with hydrogen peroxide in the evening while plants were treated in the morning in the first set and the reciprocal replicates (^{14}N treated/^{15}N control) within the same experiment were consistent (data not shown). Some reports indicate that light is required for the induction of some PR-proteins after infection (Zeier et al., 2004) and this might explain the variation in the induction between these two experiments.

For quantitative analysis of whole proteomes, automation of data analysis was required. The automated method that was designed for large-scale data mining provided an easy-to-use

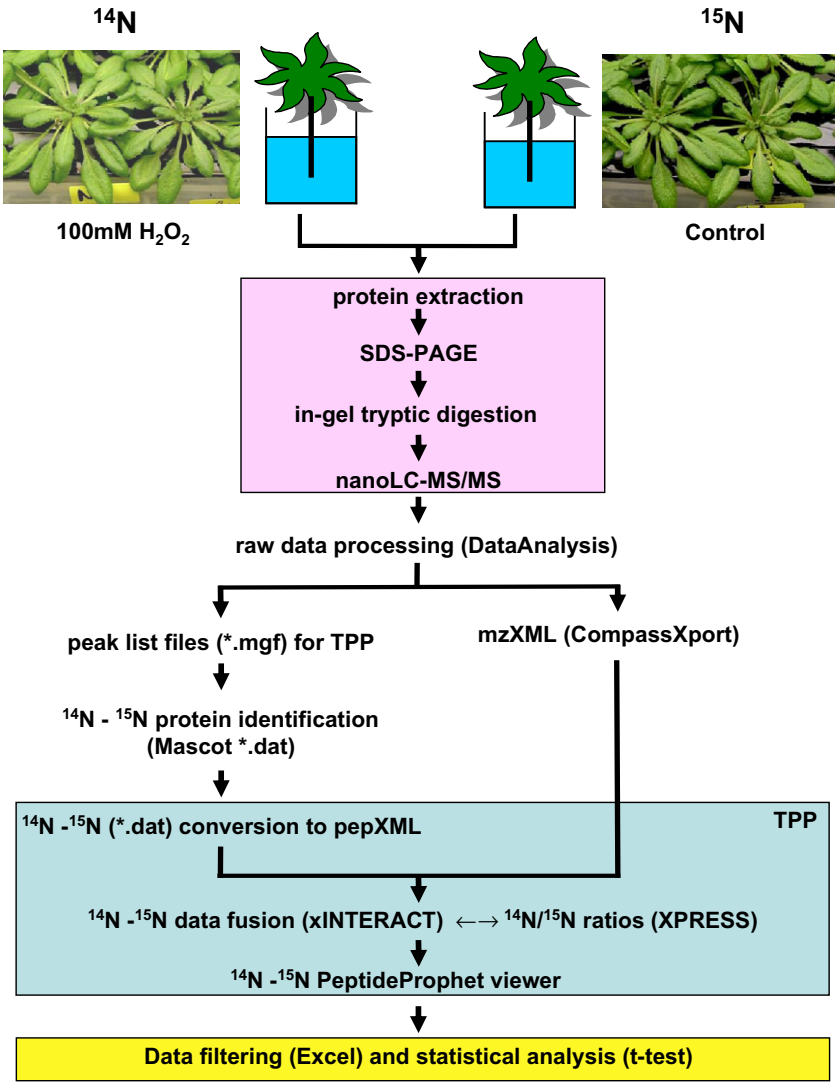

Fig. 6. Typical analytical workflow for quantitative proteomics using HILEP in combination with MS analysis. $^{14}N/^{15}N$ peptide ratio calculation from identified proteins was automated using the trans-proteomic pipeline interface (TPP). See text for details.

workflow, allowing statistical analysis for high statistical confidence and the discrimination between sequence specific isoforms. Protein ratios measured manually were compared to data retrieved with the automated quantitation pipeline, and showed consistency between the manual and the automated quantitation method for the same dataset and between experimental replicates. The lack of statistical significance for some quantitated proteins correlated with the low number of peptide ratios measured for these proteins and the resulting large SD. However, statistical errors can be reduced by increasing the number of quantified peptides. Nonetheless, variation between biological samples has been observed to be greater than the SD due to peptide ratio measurement error within a single protein (not shown).

In some cases, manual data validation might still be necessary to avoid quantitation errors (Kolkman et al., 2006) due to overlapping ion species. As shown in this study, analysis of the ^{14}N and ^{15}N isotope patterns will naturally help in detecting these undesirable convoluted ion signals, for which FTICR–MS can provide the high resolving power needed to distinguish the different overlapping ion signals at the same nominal m/z values. To keep the advantage of fast MS/MS data acquisition, when hybrid ion trap-FTICR or orbitrap instruments (Makarov et al., 2006) are not available, ion trap MS/MS data for protein identification and FTICR–MS data for protein quantitation can be combined to improve quantitative protein measurements with reduced SD, by aligning LC–MS and LC–MS/MS datasets acquired following identical LC runs (Palmblad et al., 2007). Similar levels of precision to those achieved in our study have been shown in large-scale protein quantitation studies of prokaryotic systems using metabolic $^{14}N/^{15}N$-labelling that has been performed exclusively with FTICR (Conrads et al., 2001; Smith et al., 2001) as well as with a 3D ion trap (Kolkman et al., 2006) or a hybrid ion-trap FTICR (Benschop et al., 2007).

Due to the uniform labelling of every amino acid residue, ^{15}N metabolic labelling is readily applicable to quantify virtually any post-transcriptional modification (PTM) as it has been applied to early phosphorylation events in differentially elicited *Arabidopsis* cell cultures (Benschop et al., 2007). For instance HILEP could be applied for the quantitation of PTMs of proteins that are known to be post-transcriptionally modified during oxidative and nitrositive stress in plants (Lindermayr et al., 2005; Zaffagnini et al., 2007). However, to allow discrimination with high statistical confidence between isoforms with the same amino acid sequences but with different PTMs, 2D gel protein fractionation should be combined with HILEP to resolve such protein isoforms (Jones et al.,

2006), thus avoiding the mass spectrometric quantitation of proteins based on a single phosphopeptide detection (Benschop et al., 2007). Metabolic ^{15}N-labelling can also be used for the subcellular location of proteins in a similar way to LOPIT (Localization of Organelle proteins by Isotope Tagging) with iTRAQ labelling (Dunkley et al., 2004).

The use of two stable isotopes, such as ^{13}C in combination with ^{15}N, could allow multiplexing (Snijders et al., 2005). Nevertheless the use of ^{13}C is experimentally not as simple as ^{15}N for photoautotrophic plants. However, partial labelling such as in the "subtle modification of isotope ratio proteomics" technique (SMIRP) (Whitelegge et al., 2004) can be easily applied using ^{13}C metabolic isotope labelling. Achieving as little as 6% ^{13}C, incorporation, the isotope envelope pattern is sufficiently affected that it can be used for quantitation of peptides. However, isotope envelopes of a "normal" ^{12}C peptide and a 6% ^{13}C peptide typically overlap, leading to similar problems as with partial ^{15}N-labelling and thus requiring mathematical interpretation, i.e. deconvolution.

Finally, as the analytical workflow allowed the discrimination between protein isoforms from different gene loci, the use of this quantitative proteomics method might unravel the complexity of differential induction of proteins belonging to the same gene families, without the absolute requirement of 2D-gel fractionation and image analysis. For instance, this has been illustrated in the present study by the differential expression of two β-glucosidase and two β-xylosidase isoforms in the IWFs.

In conclusion, we have applied metabolic ^{15}N-labelling to whole plants grown under hydroponic conditions, demonstrated its analytical potential in a biological experiment and obtained results consistent with earlier non-proteomic studies. With automated data processing as applied in this study, whole plant proteomic experiments are feasible at the large-scale, high-throughput level even when HILEP is used in combination with optimised protein pre-fractionation and high-resolution mass spectrometry. Due to its cost-effectiveness and the inherent advantages of plant metabolism, multiplexing will be a practical option as will be the large-scale labelling of organisms feeding on labelled plants and other organisms further up in the food chain.

Thus, we have demonstrated that HILEP is a simple and robust metabolic labelling technique, and in combination with mass spectrometry, an easy-to-use and automatable methodology for reliable quantitation of protein expression down to the isoform level in global proteome analyses.

4. Experimental

4.1. Hydroponic isotope labelling of entire plants (HILEP)

Arabidopsis thaliana ecotype Columbia Col-0 seeds were sterilised (Noren et al., 2004) and vernalised 48 h at 4 °C. Transparent and sterile 200 µl tip boxes were used as mini-greenhouses for germination. One seed was sown on each unsealed tip containing half-strength hydroponic medium and 0.7% agar (Fluka, Gillingham, UK). The boxes were sealed with Parafilm™ and sides were wrapped in aluminium. Plants were grown under 10 h light exposure per day at 22 °C. After 10 days one third of the pipette tips were cut to allow root growth. Twelve tips containing 14 day-old plants were transferred into a perforated lid of a black painted and surface sterilised polyethylene 1 L lunch box filled with full-strength hydroponic solution. The hydroponic solution consisted of 2.5 mM KNO_3, 1 mM $CaCl_2$, 0.75 mM $MgSO_4$, 0.5 mM KH_2PO_4, 0.5 mM NH_4NO_3, 1 ml/l micronutrient solution (50 mM H_3BO_3, 10 mM $MnSO_4$ H_2O, 1.5 mM $ZnSO_4$ $7H_2O$, 1 mM $CuSO_4$ $5H_2O$, 0.58 mM MoO_3) and 1 ml/l 70 mM Fe-EDTA solution (Huttner and Bar-Zvi, 2003; Noren et al., 2004; Tocquin et al., 2003). For ^{15}N-labelling experiments, plants were grown with 99% ^{15}N-labelled KNO_3 (Cambridge Isotope Laboratories Inc., Andover MA, USA) and 98+% ^{15}N-labelled NH_4NO_3 (Sigma). Six to seven week-old plants grown in ^{14}N or ^{15}N media were sprayed with either 0.05% Tween 20 for control or with 100 mM H_2O_2 in 0.05% Tween.

4.2. Protein extraction and separation

For total extracts, leaves were collected from at least 3 plants after 20 h and 40 h and flash frozen. ^{14}N and ^{15}N leaves were pooled as a 1:1 mix (fresh weight) and ground with a mortar and pestle in liquid nitrogen and kept at −80 °C until required. Proteins were extracted in 5 volumes of ice cold 50 mM Tris pH 7.6, 0.33 M sucrose, 1 mM DTT, 1 mM $MgCl_2$, 1% (w/v) poly(vinylpolypyrrolidone) and 1/500 protease inhibitor cocktail VI (Calbiochem/Merck, Nottingham, UK). Samples were thawed, mixed and kept on ice for 5 min. Particulates were removed by two successive 10 min-centrifugations at 3300*g* and 17,860*g* at 4 °C and transferred the supernatant into a fresh tube.

For apoplastic proteins, excised leaves from 5 plants (1.0–1.5 g) were vacuum infiltrated with ice-cold 20 mM Tris, 2 mM $CaCl_2$ pH 7.5. Infiltrated leaves were gently blotted with tissue to remove excess of liquid and transferred to two 10 ml syringes without plunger placed in 50 ml tubes. Intercellular washing fluids (IWFs) were collected by a 5 min centrifugation at 693*g*. IWFs were re-centrifuged at 17,860*g* for 5 min to remove residual debris.

Protein concentrations were estimated with a Bradford reagent (Bio-Rad, Hemel Hempstead, UK). Proteins were separated on a 12% acrylamide SDS–PAGE minigel (Protean III, Bio-Rad). The gel was stained with colloidal Coomassie (Candiano et al., 2004).

4.3. In-gel tryptic digestion

Each excised gel bands was cut into 1–5 mm^3 pieces, each transferred to an individual 0.5 ml Sorenson™ microcentrifuge tube (Bioquote Ltd., York, UK) and stored at −80 °C until tryptic digestion. The gel pieces were sequentially washed, each time for 10 min, twice in 100 µl 25 mM ammonium bicarbonate (ABC), once in 50 µl 25% acetonitrile (ACN) in 25 mM ABC and twice in 30 µl 50% ACN in 25 mM ABC, followed by 20 min vacuum-drying (Eppendorf concentrator, Cambridge, UK). Cysteines were reduced by incubation at 56 °C for 45 min with 30 µl 20 mM DTT in 25 mM ABC. Excess of liquid was removed and cysteines were alkylated by incubation in darkness for 1 h with 30 µl 10 mg/mL iodoacetamide in 25 mM ABC. After three washes in 50 µl 50% ACN in 25 mM ABC the gel pieces were vacuum-dried for 20 min. The dried gel pieces were rehydrated for 15 min in 15 µl 25 mM ABC containing 8 ng/µl modified sequencing grade trypsin (Promega, Southampton, UK) prior to the addition of 15 µl 25 mM ABC and overnight incubation at 37 °C. Peptides were extracted 3 times with 30 µl 50% ACN in 5% TFA and once with 90% ACN in 1% TFA. Extracts were pooled, vacuum-dried and kept at −80 °C until further analysis.

4.4. Protein identification by mass spectrometry

Peptides were reconstituted in 20 µl 0.2% TFA, separated by LC using a Dionex Ultimate™ HPLC system (LC Packings/Dionex, Amsterdam, The Netherlands) as previously described (Palmblad et al., 2007), but with a flow rate of 250 nL/min. The HPLC system was coupled to either an Esquire HCT ion trap (Bruker Daltonics, Bremen, Germany) or a 7 tesla Apex Qe–FTICR–MS (Bruker Daltonics). Peptides identified by MS/MS with the FTICR were used for enhanced m/z calibration (Palmblad et al., 2006). Calculated exact masses of peptides identified in the ion trap were sufficient to retrieve corresponding mass spectra from the LC–FTICR data without chromatographic alignment.

Raw LC–MS/MS data were batch-processed in DataAnalysis 3.3.147 (Bruker Daltonics http://www.bruker.com). Up to 2000 compounds (retention time restriction of 5–110 min) with a signal-to-noise ratio above 5 were extracted and exported as Mascot Generic Files (MGF). For protein identification, MGF files were submitted to Mascot searching using Daemon 2.1 (Matrix Science; http://www.matrixscience.com) on an in-house Mascot server 2.1.04 (Perkins et al., 1999). The data was searched twice: once with the normal ^{14}N masses and once with the labelled ^{15}N masses, against the EBI *Arabidopsis thaliana* FASTA protein database (20070220), tolerating a 1.2 Da error in MS and a 0.4 Da error in MS/MS, up to two tryptic missed cleavages and submitting 2^+ and 3^+ charged ions. Cysteine carbamidomethylation was set as a permanent modification, methionine oxidation and proline hydroxylation were included as variable modifications.

4.5. Manual calculation of relative protein abundance using $^{15}N/^{14}N$ ratios

Manual protein quantitation was restricted to identified proteins with a minimum Mascot score corresponding to a confidence level of 95%, a minimum of 3 matching unique peptides per protein and with at least one peptide of the highest rank (i.e. being the most likely assignment of the MS/MS spectrum and belonging to the protein with the highest Mascot score of all protein hits containing this peptide) and peptide ion score greater than the identity score (95%). The associated gene locus number of the protein was retrieved from the TIGR database (http://www.tigr.org) or NCBI websites (http://www.ncbi.nlm.nih.gov/entrez/query).

The m/z value, the charge and the chromatographic elution time of the peptides to quantify were retrieved from the Mascot search results allowing the identification of the corresponding chromatographic peak. As ^{14}N ions and their corresponding ^{15}N ions co-elute, mass spectra were averaged over the time interval defined by their chromatographic peak. The ^{14}N and ^{15}N isotope envelopes were manually examined to eliminate overlapping species. The mass difference between the most abundant peaks in both ^{14}N and ^{15}N envelopes was correlated to the number of nitrogen atoms deduced from the amino acid sequence. For ion trap MS data, the relative amount of corresponding peptide pairs was calculated as the $^{14}N/^{15}N$ ratio of the sums of the isotope peak areas of the distinct ^{15}N and ^{14}N envelopes. Isotope peak intensities rather than peak areas were used for the FTICR–MS data. Statistical significance (95%) was evaluated by the Student's t-test.

4.6. Automation of protein quantitation

Data were analysed automatically as described in Annex S4 and summarised in Fig. 6. In brief, raw LC–MS/MS data sets were processed with DataAnalysis 3.3.147 (Bruker Daltonics) for peak and compound detection, deconvolution and the export of peak lists in a Mascot Generic Format (MGF, *.mgf). In parallel, raw LC–MS/MS datasets were converted to mzXML file format (*.mzXML) using CompassXport 1.3.1 (Bruker Daltonics). Using Daemon 2.1 (Matrix Science), all MGF files were submitted twice to Mascot for ^{14}N or ^{15}N protein identification, respectively. Each Mascot result file ("*.dat") was automatically renamed to match the corresponding raw data file name and converted to a pepXML file with the Mascot2XML tool (trans-proteomic pipeline 2.9.5, TPP; http://tools.proteomecenter.org/software.php; (Keller et al., 2005)). In TPP, all the ^{14}N pepXML files were merged with the xINTERACT tool to calculate $^{14}N/^{15}N$ peptide ratios with XPRESS. Individual protein identifications and peptide ratios were retrieved and filtered with the pepXML viewer PeptideProphet. All processes were repeated for ^{15}N files. For high identification confidence and in order to distinguish between database entry isoforms (proteins from different gene loci), peptides with an ion score higher than the identity score were exported to an Excel worksheet and further filtered using the in-house written "pepXML2Excel" (Annex S4) AWK script (Aho et al., 1988) to retrieve proteins identified and quantified with at least three distinct unique peptides solely assigned to a single database entry isoform. ^{14}N and ^{15}N INTERACT ("*.XML") data were merged and visualized in the TPP ProteinProphet viewer for examination of protein identification probabilities of the combined ^{14}N and ^{15}N Mascot search results. However, ProteinProphet was not used for peptide quantitation as it was not directly applicable to the statistical analysis of protein ratios.

To evaluate the significance of each relative protein quantitation result, a two-sided heteroscedastic (Welsch's) t-test was applied to test each null hypothesis that the observed ratios for the peptides associated with a protein have the same distribution as a large number of peptides from the Rubisco large subunit (AtCg00490), an abundant protein whose relative ratios did not vary in these experiments.

Acknowledgements

The authors would like to thanks their colleagues Trevor Gibson and Davinia Mills for technical support in mass spectrometry and the critical reading of the manuscript.

Appendix A. Supplementary material

Supplementary data associated with this article can be found, in the online version, at doi:10.1016/j.phytochem.2008.04.007.

References

Aho, A.V., Kernighan, B.W., Weinberger, P.J., 1988. The AWK Programming Language. Addison-Wesley.

Apel, K., Hirt, H., 2004. Reactive oxygen species: metabolism, oxidative stress, and signal transduction. Annu. Rev. Plant Biol. 55, 373–399.

Baxter, C.J., Redestig, H., Schauer, N., Repsilber, D., Patil, K.R., Nielsen, J., Selbig, J., Liu, J., Fernie, A.R., Sweetlove, L.J., 2007. The metabolic response of heterotrophic *Arabidopsis* cells to oxidative stress. Plant Physiol. 143, 312–325.

Benschop, J.J., Mohammed, S., O'Flaherty, M., Heck, A.J., Slijper, M., Menke, F.L., 2007. Quantitative phosphoproteomics of early elicitor signaling in *Arabidopsis*. Mol. Cell Proteomics 6, 1198–1214.

Bindschedler, L.V., Dewdney, J., Blee, K.A., Stone, J.M., Asai, T., Plotnikov, J., Denoux, C., Hayes, T., Gerrish, C., Davies, D.R., Ausubel, F.M., Paul Bolwell, G., 2006. Peroxidase-dependent apoplastic oxidative burst in *Arabidopsis* required for pathogen resistance. Plant J. 47, 851–863.

Candiano, G., Bruschi, M., Musante, L., Santucci, L., Ghiggeri, G.M., Carnemolla, B., Orecchia, P., Zardi, L., Righetti, P.G., 2004. Blue silver: a very sensitive colloidal Coomassie G-250 staining for proteome analysis. Electrophoresis 25, 1327–1333.

Chivasa, S., Hamilton, J.M., Pringle, R.S., Ndimba, B.K., Simon, W.J., Lindsey, K., Slabas, A.R., 2006. Proteomic analysis of differentially expressed proteins in fungal elicitor-treated *Arabidopsis* cell cultures. J. Exp. Bot. 57, 1553–1562.

Conrads, T.P., Alving, K., Veenstra, T.D., Belov, M.E., Anderson, G.A., Anderson, D.J., Lipton, M.S., Pasa-Tolic, L., Udseth, H.R., Chrisler, W.B., Thrall, B.D., Smith, R.D., 2001. Quantitative analysis of bacterial and mammalian proteomes using a combination of cysteine affinity tags and ^{15}N-metabolic labeling. Anal. Chem. 73, 2132–2139.

Dong, X., Mindrinos, M., Davis, K.R., Ausubel, F.M., 1991. Induction of *Arabidopsis* defense genes by virulent and avirulent Pseudomonas syringae strains and by a cloned avirulence gene. Plant Cell 3, 61–72.

Dunkley, T.P., Watson, R., Griffin, J.L., Dupree, P., Lilley, K.S., 2004. Localization of organelle proteins by isotope tagging (LOPIT). Mol. Cell Proteomics 3, 1128–1134.

Engelsberger, W.R., Erban, A., Kopka, J., Schulze, W.X., 2006. Metabolic labeling of plant cell cultures with $K_{15}NO_3$ as a tool for quantitative analysis of proteins and metabolites. Plant Methods 2, 14.

Fang, R., Elias, D.A., Monroe, M.E., Shen, Y., McIntosh, M., Wang, P., Goddard, C.D., Callister, S.J., Moore, R.J., Gorby, Y.A., Adkins, J.N., Fredrickson, J.K., Lipton, M.S., Smith, R.D., 2006. Differential label-free quantitative proteomic analysis of Shewanella oneidensis cultured under aerobic and suboxic conditions by accurate mass and time tag approach. Mol. Cell Proteomics 5, 714–725.

Gerber, S.A., Rush, J., Stemman, O., Kirschner, M.W., Gygi, S.P., 2003. Absolute quantification of proteins and phosphoproteins from cell lysates by tandem MS. Proc. Natl. Acad. Sci. USA 100, 6940–6945.

Gorecka, K.M., Konopka-Postupolska, D., Hennig, J., Buchet, R., Pikula, S., 2005. Peroxidase activity of annexin 1 from *Arabidopsis thaliana*. Biochem. Biophys. Res. Commun. 336, 868–875.

Gruhler, A., Schulze, W.X., Matthiesen, R., Mann, M., Jensen, O.N., 2005. Stable isotope labeling of *Arabidopsis thaliana* cells and quantitative proteomics by mass spectrometry. Mol. Cell Proteomics 4, 1697–1709.

Heck, A.J., Krijgsveld, J., 2004. Mass spectrometry-based quantitative proteomics. Expert Rev. Proteomics 1, 317–326.

Hirner, A., Ladwig, F., Stransky, H., Okumoto, S., Keinath, M., Harms, A., Frommer, W.B., Koch, W., 2006. *Arabidopsis* LHT1 is a high-affinity transporter for cellular amino acid uptake in both root epidermis and leaf mesophyll. Plant Cell 18, 1931–1946.

Huttlin, E.L., Hegeman, A.D., Harms, A.C., Sussman, M.R., 2007. Comparison of full versus partial metabolic labeling for quantitative proteomics analysis in *Arabidopsis thaliana*. Mol. Cell Proteomics 6, 860–881.

Huttner, D., Bar-Zvi, D., 2003. An improved, simple, hydroponic method for growing *Arabidopsis thaliana*. Plant Mol. Biol. Reporter 21, 59–63.

Ippel, J.H., Pouvreau, L., Kroef, T., Gruppen, H., Versteeg, G., van den Putten, P., Struik, P.C., van Mierlo, C.P., 2004. In vivo uniform (15)N-isotope labelling of plants: using the greenhouse for structural proteomics. Proteomics 4, 226–234.

Jones, A.M., Thomas, V., Bennett, M.H., Mansfield, J., Grant, M., 2006. Modifications to the *Arabidopsis* defense proteome occur prior to significant transcriptional change in response to inoculation with Pseudomonas syringae. Plant Physiol. 142, 1603–1620.

Keller, A., Eng, J., Zhang, N., Li, X.J., Aebersold, R., 2005. A uniform proteomics MS/MS analysis platform utilizing open XML file formats. Mol. Syst. Biol. 1, 0017.

Kolkman, A., Daran-Lapujade, P., Fullaondo, A., Olsthoorn, M.M., Pronk, J.T., Slijper, M., Heck, A.J., 2006. Proteome analysis of yeast response to various nutrient limitations. Mol. Syst. Biol. 2, 0026.

Krijgsveld, J., Ketting, R.F., Mahmoudi, T., Johansen, J., Artal-Sanz, M., Verrijzer, C.P., Plasterk, R.H., Heck, A.J., 2003. Metabolic labeling of *C. elegans* and *D. melanogaster* for quantitative proteomics. Natl. Biotechnol. 21, 927–931.

Lindermayr, C., Saalbach, G., Durner, J., 2005. Proteomic identification of *S*-nitrosylated proteins in *Arabidopsis*. Plant Physiol. 137, 921–930.

Makarov, A., Denisov, E., Kholomeev, A., Baischun, W., Lange, O., Strupat, K., Horning, S., 2006. Performance evaluation of a hybrid linear ion trap/orbitrap mass spectrometer. Anal. Chem. 78, 2113–2120.

Mann, M., 2006. Functional and quantitative proteomics using SILAC. Natl. Rev. Mol. Cell Biol. 7, 952–958.

Marouga, R., David, S., Hawkins, E., 2005. The development of the DIGE system: 2D fluorescence difference gel analysis technology. Anal. Bioanal. Chem. 382, 669–678.

McCabe, M.S., Garratt, L.C., Schepers, F., Jordi, W.J., Stoopen, G.M., Davelaar, E., van Rhijn, J.H., Power, J.B., Davey, M.R., 2001. Effects of P (SAG12)-IPT gene expression on development and senescence in transgenic lettuce. Plant Physiol 127, 505–516.

Neill, S., Desikan, R., Hancock, J., 2002. Hydrogen peroxide signalling. Curr. Opin. Plant Biol. 5, 388–395.

Nelson, C.J., Huttlin, E.L., Hegeman, A.D., Harms, A.C., Sussman, M.R., 2007. Implications of ^{15}N-metabolic labeling for automated peptide identification in *Arabidopsis thaliana*. Proteomics 7, 1279–1292.

Noren, H., Svensson, P., Andersson, B., 2004. A convenient and versatile hydroponic cultivation system for *Arabidopsis thaliana*. Physiologia Plantarum 121, 343–348.

Ott, P.G., Varga, G.J., Szatmari, A., Bozso, Z., Klement, E., Medzihradszky, K.F., Besenyei, E., Czelleng, A., Klement, Z., 2006. Novel extracellular chitinases rapidly and specifically induced by general bacterial elicitors and suppressed by virulent bacteria as a marker of early basal resistance in tobacco. Mol. Plant Microbe Interact 19, 161–172.

Palmblad, M., Bindschedler, L.V., Cramer, R., 2007. Quantitative proteomics using uniform (15)N-labeling, MASCOT, and the trans-proteomic pipeline. Proteomics 7, 3462–3469.

Palmblad, M., Bindschedler, L.V., Gibson, T.M., Cramer, R., 2006. Automatic internal calibration in liquid chromatography/Fourier transform ion cyclotron resonance mass spectrometry of protein digests. Rapid Commun. Mass Spectrom. 20, 3076–3080.

Palmblad, M., Buijs, J., Hakansson, P., 2001. Automatic analysis of hydrogen/deuterium exchange mass spectra of peptides and proteins using calculations of isotopic distributions. J. Am. Soc. Mass Spectrom. 12, 1153–1162.

Palmblad, M., Cramer, R., 2007. Liquid matrix deposition on conductive hydrophobic surfaces for tuning and quantitation in UV–MALDI mass spectrometry. J. Am. Soc. Mass Spectrom. 18, 693–697.

Perkins, D.N., Pappin, D.J., Creasy, D.M., Cottrell, J.S., 1999. Probability-based protein identification by searching sequence databases using mass spectrometry data. Electrophoresis 20, 3551–3567.

Ross, A., Kessler, W., Krumme, D., Menge, U., Wissing, J., van den Heuvel, J., Flohe, L., 2004a. Optimised fermentation strategy for ^{13}C/^{15}N recombinant protein labelling in *Escherichia coli* for NMR-structure analysis. J. Biotechnol. 108, 31–39.

Ross, P., Dey, S., Pillai, S., Daniels, S., Williamson, B., Guertin, S., Minkoff, M., Chen, X., Purkayastha, B., Pappin, D, 2006. Protein quantitation using a novel 8-plex set of isobaric peptide labels. 54th ASMS Conference, Seattle, WA. ThP 62512.

Ross, P.L., Huang, Y.N., Marchese, J.N., Williamson, B., Parker, K., Hattan, S., Khainovski, N., Pillai, S., Dey, S., Daniels, S., Purkayastha, S., Juhasz, P., Martin, S., Bartlet-Jones, M., He, F., Jacobson, A., Pappin, D.J., 2004b. Multiplexed protein quantitation in *Saccharomyces cerevisiae* using amine-reactive isobaric tagging reagents. Mol. Cell Proteomics 3, 1154–1169.

Schmidt, A., Kellermann, J., Lottspeich, F., 2005. A novel strategy for quantitative proteomics using isotope-coded protein labels. Proteomics 5, 4–15.

Smith, R.D., Pasa-Tolic, L., Lipton, M.S., Jensen, P.K., Anderson, G.A., Shen, Y., Conrads, T.P., Udseth, H.R., Harkewicz, R., Belov, M.E., Masselon, C., Veenstra, T.D., 2001. Rapid quantitative measurements of proteomes by Fourier transform ion cyclotron resonance mass spectrometry. Electrophoresis 22, 1652–1668.

Snijders, A.P., de Vos, M.G., Wright, P.C., 2005. Novel approach for peptide quantitation and sequencing based on ^{15}N and ^{13}C metabolic labeling. J. Proteome Res. 4, 578–585.

Tang, K., Page, J.S., Smith, R.D., 2004. Charge competition and the linear dynamic range of detection in electrospray ionization mass spectrometry. J. Am. Soc. Mass. Spectrom. 15, 1416–1423.

Tocquin, P., Corbesier, L., Havelange, A., Pieltain, A., Kurtem, E., Bernier, G., Perilleux, C., 2003. A novel high efficiency, low maintenance, hydroponic system for synchronous growth and flowering of *Arabidopsis thaliana*. BMC Plant Biol. 3, 2.

Unlu, M., Morgan, M.E., Minden, J.S., 1997. Difference gel electrophoresis: a single gel method for detecting changes in protein extracts. Electrophoresis 18, 2071–2077.

van Loon, L.C., Rep, M., Pieterse, C.M.J., 2006. Significance of inducible defense-related proteins in infected plants. Ann. Rev. Phytopathol. 44, 135–162.

Whitelegge, J.P., Katz, J.E., Pihakari, K.A., Hale, R., Aguilera, R., Gomez, S.M., Faull, K.F., Vavilin, D., Vermaas, W., 2004. Subtle modification of isotope ratio proteomics; an integrated strategy for expression proteomics. Phytochemistry 65, 1507–1515.

Wienkoop, S., Weckwerth, W., 2006. Relative and absolute quantitative shotgun proteomics: targeting low-abundance proteins in *Arabidopsis thaliana*. J. Exp. Bot. 57, 1529–1535.

Wu, C.C., MacCoss, M.J., Howell, K.E., Matthews, D.E., Yates 3rd, J.R., 2004. Metabolic labeling of mammalian organisms with stable isotopes for quantitative proteomic analysis. Anal. Chem. 76, 4951–4959.

Yi, E.C., Li, X.J., Cooke, K., Lee, H., Raught, B., Page, A., Aneliunas, V., Hieter, P., Goodlett, D.R., Aebersold, R., 2005. Increased quantitative proteome coverage with (13)C/(12)C-based, acid-cleavable isotope-coded affinity tag reagent and modified data acquisition scheme. Proteomics 5, 380–387.

Zaffagnini, M., Michelet, L., Marchand, C., Sparla, F., Decottignies, P., Le Marechal, P., Miginiac-Maslow, M., Noctor, G., Trost, P., Lemaire, S.D., 2007. The thioredoxin-independent isoform of chloroplastic glyceraldehyde-3-phosphate dehydrogenase is selectively regulated by glutathionylation. FEBS J. 274, 212–226.

Zeier, J., Pink, B., Mueller, M.J., Berger, S., 2004. Light conditions influence specific defence responses in incompatible plant–pathogen interactions: uncoupling systemic resistance from salicylic acid and PR-1 accumulation. Planta 219, 673–683.